UEF//eRepository

DSpace **https://erepo.uef.fi**

Rinnakkaistallenteet Terveystieteiden tiedekunta

2017

Amyloid Plaques Show Binding Capacity of Exogenous Injected Amyloid-ß

Gureviciene Irina

IOS Press

Tieteelliset aikakauslehtiartikkelit
© IOS Press and the authors
All rights reserved
http://dx.doi.org/10.3233/JAD-160453

https://erepo.uef.fi/handle/123456789/7893
Downloaded from University of Eastern Finland's eRepository

Amyloid plaques show binding capacity of exogenous injected Aβ

Irina Gureviciene[a]*, Kestutis Gurevicius[a], Ekaterina Mugantseva[b,c], Mikhail Kislin[b], Leonard Khiroug[b,d], Heikki Tanila[a]

[a] A. I. Virtanen Institute, University of Eastern Finland, Kuopio, Finland

[b] Neuroscience Center, University of Helsinki, Helsinki, Finland

[c] Institute of Theoretical & Experimental Biophysics, RAS, Pushchino, Russia

[d] Neurotar Ltd, Helsinki Finland, ***www.neurotar.com***

*Correspondence to:

Irina Gureviciene, Ph.D.

Department of Neurobiology

A.I.Virtanen Institute for Molecular Sciences

University of Eastern Finland (Kuopio Campus)

Bioteknia 1 (Neulaniementie 2)

P.O.Box 1627

70211 Kuopio

Finland

Phone: + 358 505265084

Fax: + 358 17 163030

E-mail: Irina.Gureviciene@uef.fi

Key words

Alzheimer's disease, amyloid-β, *in vivo* imaging, transgenic, multiphoton

Acknowledgement

We thank Dr. David Borchelt (University of Florida, FL, USA) and Joanna Jankowsky (Baylor College of Medicine, Houston, TX, USA) for the APP/PS1 breeder mice. This study was supported by European Union 7th Framework Programme grant HEALTH-2007-MEMOLOAD (201159), Academy of Finland, and CIMO Finland.

Abstract

Amyloid plaques, although inducing damage to the immediately surrounding neuropil, have been proposed to provide a relatively innocuous way to deposit toxic soluble amyloid-β (Aβ) species. Here we address this hypothesis by exploring spread and absorption of fluorescent Aβ to pre-existing amyloid plaques after local application in wild-type mice vs. APP/PS1 transgenic mice with amyloid plaques. Local intracortical or intracerebroventricular injection of fluorescently labeled Aβ in APP/PS1 mice with a high plaque density resulted in preferential accumulation of the peptide in amyloid plaques in both conventional post-mortem histology and in live imaging using two-photon microscopy. These findings support the contention that amyloid plaques may act as buffers to protect neurons from the toxic effects of momentary high concentrations of soluble Aβ oligomers.

Introduction

Amyloid-β (Aβ) is the key protein in the pathogenesis of Alzheimer disease (AD). It is present in the brain in different soluble or insoluble forms. During AD pathogenesis, soluble Aβ aggregates into oligomers and insoluble extracellular amyloid plaques (Yan et al., 2009). Furthermore, amyloid deposition can be either within the brain parenchyma (plaques) or in association with the brain blood vessels (cerebral amyloid angiopathy). To date, amyloid plaques remain the primary markers of brain pathology in AD, although their exact role in the disease pathogenesis is still unclear. On the one hand, dystrophy (Wong et al., 1999) or destruction [the EM ref given by Reviewer #2] of neural elements can be seen around amyloid plaques,

Wong TP, Debeir T, Duff K, Cuello AC. Reorganization of cholinergic terminals in the cerebral cortex and hippocampus in transgenic mice carrying mutated presenilin-1 and amyloid precursor protein transgenes. J Neurosci. 1999 Apr 1;19(7):2706-16.

and amyloid load in the medial temporal lobe correlates with volume loss of hippocampus (Mormino et al., 2009). On the other hand, despite the central role of amyloid plaques in AD pathology, most studies have failed to find a correlation between amyloid plaque load in AD brains and cognitive performance (Terry et al., 1991; Villemagne et al., 2011). Further, accumulating evidence indicates that soluble oligomeric and fibrillar forms of Aβ play an essential role in disrupting plasticity mechanisms causing memory impairment and accelerating the formation of neurofibrillary tangles that eventually cause synaptic failure and neuronal death (Barghorn et al., 2005; Brouillette et al., 2012; Cleary et al., 2005; Dahlgren et al., 2002; Klein et al., 2001; Lambert et al., 1998; Lesne et al., 2006; Lorenzo and Yankner, 1994; Selkoe, 2008; Townsend et al., 2006; Zempel et al., 2010). It is also generally agreed that synapse - in particular, its postsynaptic compartment - is the primary target of Aβ (Masliah, 1995; Selkoe, 2002; Tanzi, 2005; Walsh and Selkoe, 2004). Thus the AD research community is moving away from the original idea that amyloid plaques are the culprits of the disease and assign this role more to the soluble oligomers. It has also been suggested that amyloid plaques provide a mechanism for the brain to get rid of soluble toxic Aβ oligomers (Selkoe & Hardy, 2016). However, little is known about the interaction of soluble Aβ aggregates and amyloid plaques *in vivo*. Whereas early *in vivo* imaging studies in amyloid plaques bearing transgenic mice suggested rapid expansion and growth arrest of amyloid plaques (Christie et al., 2001), later studies have shown that amyloid plaque growth only slows down in aged animals, but never completely halts (Burgold et al., 2011; Condello et al., 2011; Hefendehl et al., 2011; Yan et al., 2009). This view implies that plaques should possess binding capacity for additional Aβ.

Here we directly explored the hypothesis that amyloid plaques could bind soluble toxic oligomers. We injected fluorescently labeled Aβ locally into the neocortex or into the cerebral ventricle and followed up its distribution over 24 h employing both conventional post-mortem histology and *in vivo* two-photon imaging techniques. Collectively, our data lend support to the idea that amyloid plaques have remaining buffering capacity to soluble toxic Aβ species.

Materials and Methods

1. ANIMALS

Adult female heterozygous APPswe/PS1dE9 transgenic (later briefly TG) mice and their nontransgenic littermates (later referred to as wild-type mice, WT) were used in this study. APPswe/PS1dE9 colony founders were obtained from D. Borchelt and J. Jankowsky (Johns Hopkins University, Baltimore, MD, USA). This strain expresses mouse APP695 harboring a human Aβ domain and mutations K595N and M596L linked to Swedish familial AD pedigrees, and human PS1-dE9 (deletion of exon 9) vectors controlled by independent mouse prion protein promoter elements. The two transgenes co-integrate and co-segregate as a single locus (Jankowsky et al., 2004). The line was originally maintained on a hybrid background, mice from the local colony at the University of Eastern Finland were backcrossed for 13 generations to C57BL/6J mice. Notably, the time course of amyloid pathology is similar in the mouse line kept on a C57BL/6J x C3H hybrid background (Garcia-Alloza et al., 2006) as our backcrossed C57BL/6J line (Minkeviciene et al., 2008; Shemer et al., 2006). In this mouse line amyloid plaques start to appear at 3-4 months of age in the cortex and the hippocampus (Garcia-Alloza et al., 2006; Shemer et al., 2006) and show an exponential increase until ~10 months of age. Throughout the experiments, animals were group-housed in a controlled environment (temperature, 21 ± 1 °C; humidity, 50 ± 10 %; light period, 7:00 A.M. to 7:00 P.M.) and had *ad libitum* access to food and water. Experiments were conducted in accordance with the European Communities Directive (86/609/EEC), and approved by the Animal Experimental Board of Finland.

2. TWO-PHOTON IN VIVO IMAGING

Cranial window surgery. Nine- to 10-month-old mice were anesthetized with an i.p. injection of ketamine (100 mg/kg) + xylazine (10.0 mg/kg). A cranial window over the right cortical hemisphere was surgically implanted as described previously (Holtmaat et al., 2009). First, a circular piece of the skull (4 mm in diameter; centered over the parietal bone, approx. 5.5 mm caudal from bregma and 5.5 mm lateral of the midline) was removed using a high-speed dental drill (Foredom Co, Bethel, CT, USA) . The brain was then covered with sterile cortical buffer (125 mM NaCl, 5 mM KCl, 10 mM glucose, 10 mM HEPES, 2 mM $CaCl_2$ and 2 mM $MgSO_4$ in distilled H_2O). Second, the injections of fluorescently labeled Aβ1-42 (red-fluorescent tetramethylrhodamine azide, TAMRA-labeled; AnaSpec Inc., Fremont, CA, USA) in basic buffer (1 % NH_4OH), reconstructed by adding 50 µl of buffer to 0.1 mg of Aβ, and dilute this stock solution with 0.1 M PBS to 100 µl) in volume of 500 nl per injection, two to three injections per window, at the diagonal edges, were done before a 5 mm diameter round glass coverslip (Electron Microscopy Sciences, Hatfield, PA, USA) was glued to the skull using self-cure dental acrylic (Rapid Repair, Densply, Germany) to close the craniotomy. Third, a small custom made metal holder was glued at the top to allow fixation of the mouse head during imaging sessions. The animal remained anesthetized during surgery.

In-vivo microscopy. The two-photon imaging was performed using the FluoViewTM 1000 MP system (Olympus Europa, Hamburg, Germany). The excitation light was generated by a mode-locked Ti:Sapphire Mai-Tai DeepSee femtosecond laser (Spectra-Physics, Santa Clara, CA, USA). The laser emission was focused onto the specimen by the XLPlan N 25 x water immersion high numerical aperture (1.05) objective (Olympus Europa, Hamburg, Germany) specially designed for *in vivo* imaging. The laser wavelength of 860 nm was used for excitation of fluorescently labeled Aβ. Fluorescence was collected through the beam-splitting cube in four separate channels: 420 - 500 nm for autofluorescence detection and consequential spectral unmixing of possible "bleed-through" of autofluorescence into the Aβ channel; 515 - 560 nm for detection of second harmonic generation (SHG) signal; 590 - 650 nm for imaging of fluorescently labeled Aβ; and 660 - 740 nm. The average excitation power entering the microscope was approximately 50 mW (corresponding to 1.7 mW at the sample site) for the excitation wave length. During the imaging of the Aβ plaques at max 600 µm depth with 2 µm z-step, images were acquired at the resolution of 800 x 800 pixels per image frame (12.5 µs/pixel) to obtain more detailed pictures. To ensure better fluorescent signal stability over multiple recording sessions we normalized Aβ-TAMRA-specific channel (590 - 650 nm) by nonspecific channel (420 - 500 nm). Twenty-four hour after injection, the Aβ accumulation (increase in TAMRA fluorescent signal) in the plaque core and surrounding tissue was expressed

relatively to the signal intensity change in the parenchyma of a nonspecific channel. To ensure better fluorescent signal stability over multiple recording sessions we normalized the signal in the TAMRA-specific channel (590 - 650 nm) by dividing the signal intensity by that of the nonspecific channel (420 - 500 nm).

Image processing and data analysis. Before any additional processing, images were pre-processed to reduce noise (Median 3D filter in Fiji) (Ollion et al., 2013; Schindelin et al., 2012) and to smooth by Gaussian Blur 3D in Fiji. Amyloid plaques are known to display autofluorescence, which spans the entire visual range (Kwan et al., 2009). We used the amyloid plaque autofluorescence in the non-specific channel (420 - 500 nm, furthest away from the TAMRA fluorophore emission wavelength) for plaque detection. ImageJ (**http://rsbweb.nih.gov/ij/**) plugin '3D Roi Manager' (Ollion et al., 2013) was used for amyloid plaque detection and segmentation. All detected plaques were visually verified and only plaques > 20 µm in diameter were included in the further analysis. The 3D coordinates of the plaque surface were exported for each plaque and each time point. A custom-made MATLAB (Mathworks, Natick, MA, USA; R2008a) routine was used to match plaques recorded at the different time points. Matching was done based on the shortest Euclidean distance between plaques' centers of mass. The volume coordinates of the shell surrounding the plaque was estimated by image dilation.

3. HISTOLOGY

After the *in vivo* imaging, the mice were deeply anesthetized with ketamine (100 mg/kg) + xylazine (10.0 mg/kg), and transcardially perfused with 4 % paraformaldehyde in 0.1 M phosphate buffer (pH 7.4), and then transferred to a 30 % sucrose solution for cryoprotection. The brains were cut into coronal sections (35 µm) using a freezing, sliding microtome (Leica SM2000R, Leica Biosystems GmbH, Nussloch, Germany). Sections were mounted on gelatinized slides and coverslipped. The appropriate sections (i.e., cortical injection site, nearby areas) were digitized using an axis imager upright microscope with illumination system Colibri.2 (Carl Zeiss Microimaging GmbH, Gottingen, Germany) with 590 nm light for specific fluorescently labeled Aβ signal and with 488 nm light for nonspecific signal.

After taking the micrographs, one series was uncovered and stained using a fluorescent dye, thioflavin-S, a homogenous mixture of compounds that results from the methylation of

dehydrothiotoluidine with sulfonic acid, which is specific for the β-sheet structure, using a standard protocol (Guntern et al., 1992). Again, same sections and areas of interest were digitized using a Zeiss microscope (Carl Zeiss Microimaging GmbH, Gottingen, Germany) with 488 nm light for specific thioflavin-S signal and 590 nm light for nonspecific signal.

Results

1. *Injected fluorescently-labeled Aβ1-42 accumulates in amyloid plaques*

We hypothesized that existing plaques retain their capacity to absorb further Aβ and thus act as buffers to protect neurons from toxic soluble Aβ species. To test this hypothesis we first studied spread of fluorescent Aβ after local application in post-mortem histology. We applied 2 µl of fluorescently labelled synthetic Aβ1-42 at a concentration of 200 µM beneath the *dura mater* in an anesthetized mouse. Four hours later the animal was sacrificed and brain tissue was collected. Apart from the strong fluorescence on the brain surface (**Fig. 1** A1 & A2) the fluorescent signal was well distinguishable at least 600 µm beneath the cortical surface. Importantly, near the application site the fluorescence appeared as intensively labeled circumscribed spots that in thioflavin-S staining of the same section revealed pre-existing amyloid plaques (**Fig. 5** B1 & B2). This preferential accumulation of amyloid on the plaques was even more striking in animals sacrificed 24 h after topical application (*dura mater* removed) of fluorescent Aβ (**Fig. 2**, A1 & A2). We also tested whether Aβ penetration into the brain parenchyma and accumulation on amyloid plaques depends on the route of application. It appeared that Aβ was able to spread into the brain parenchyma and preferentially target amyloid plaques both after an intracortical microinjection (**Fig. 2**; two mice) and i.c.v injection (**Fig. 3**; two mice).

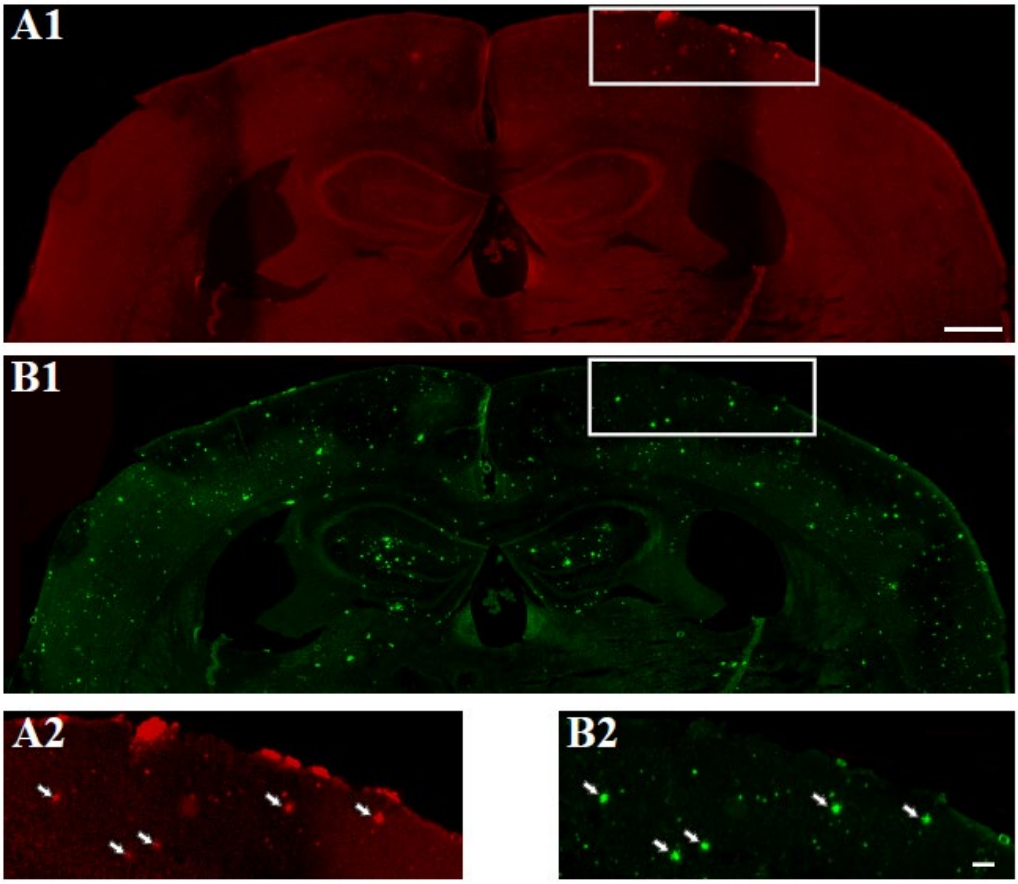

Figure 1. Histological verification that TAMRA-labeled synthetic Aβ1-42 penetrates cortex in the course of 4 h and stays attached to plaques for many hours. (A1) Red-channel fluorescence in an unstained section 4 h after topical application of labeled Aβ. (B1) The same section stained with thioflavin-S for pre-existing amyloid plaques. The white frames indicate the site of the cropped enlargements in A2 and B2. (A2) Arrows point to bright spots where fluorescently labeled Aβ1-42 accumulated near the site of application. (B2) Arrows point to the same sites as in A2 where thioflavin-S staining reveals pre-existing large plaques. Scale bar 500 µm in A1 & B1, 100 µm in B2 & A2.

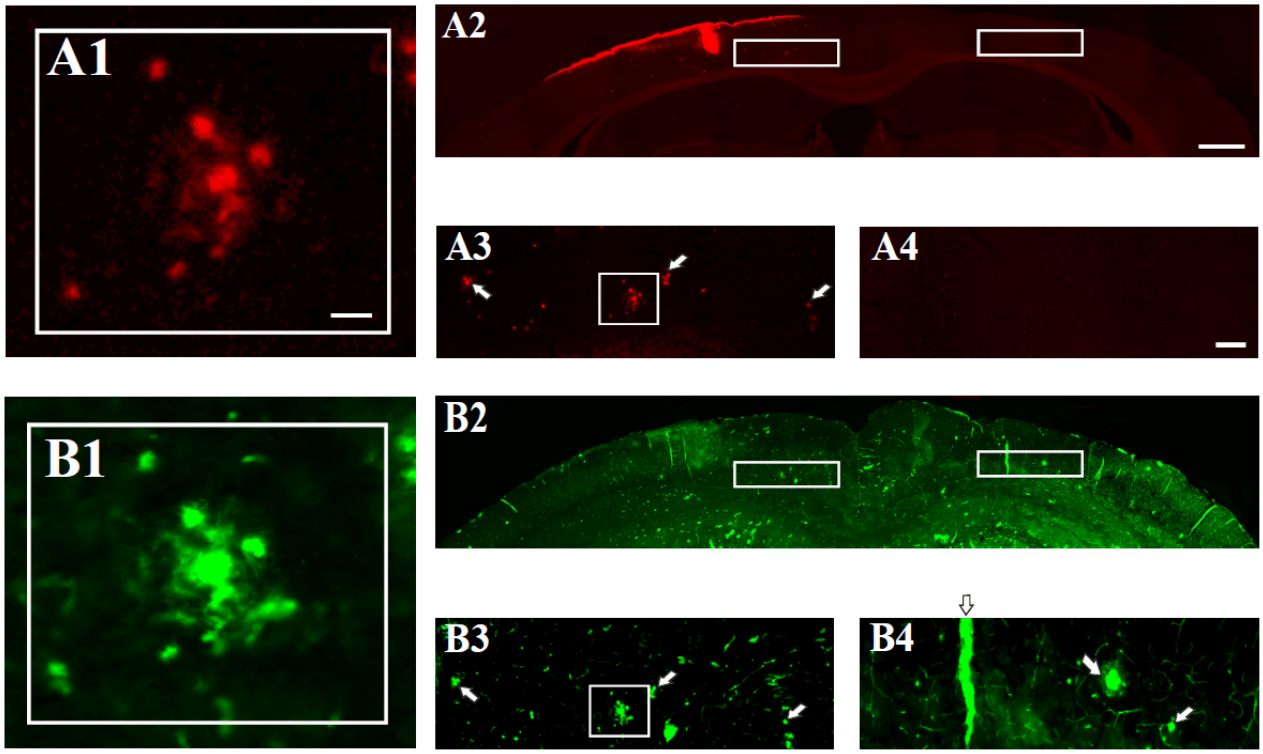

Figure 2. Representative example of spreading of TAMRA-labeled synthetic Aβ1-42 24 h after an intracortical microinjection. (A2) Panorama image (red channel, unstained) of the bilateral cortical convexity showing the injection site on the left and preferential lateral diffusion in the subarachnoidal space. The two white frames indicate the location of enlargements A3 and A4. (B2) The same section after staining with thioflavin-S. (A3) A close-up showing spotty accumulation of the TAMRA fluorescence (arrows) ipsilateral to the injection site, while a symmetric location on the contralateral site (A4) remains dark. The white frame indicates the location of a further magnification in A1. (B3) Corresponding site after thioflavin-S staining reveals pre-existing amyloid plaques (arrows). Note the presence of large plaques also on the contralateral site, as well as blood vessels with vascular amyloid (B4). (A1, B1) A close-up of a large plaque with satellites showing preferential accumulation of the TAMRA label to the plaques. Scale bar 500 µm in A2 & B2, 100 µm in A4 & B4, 10 µm in A1 & B1.

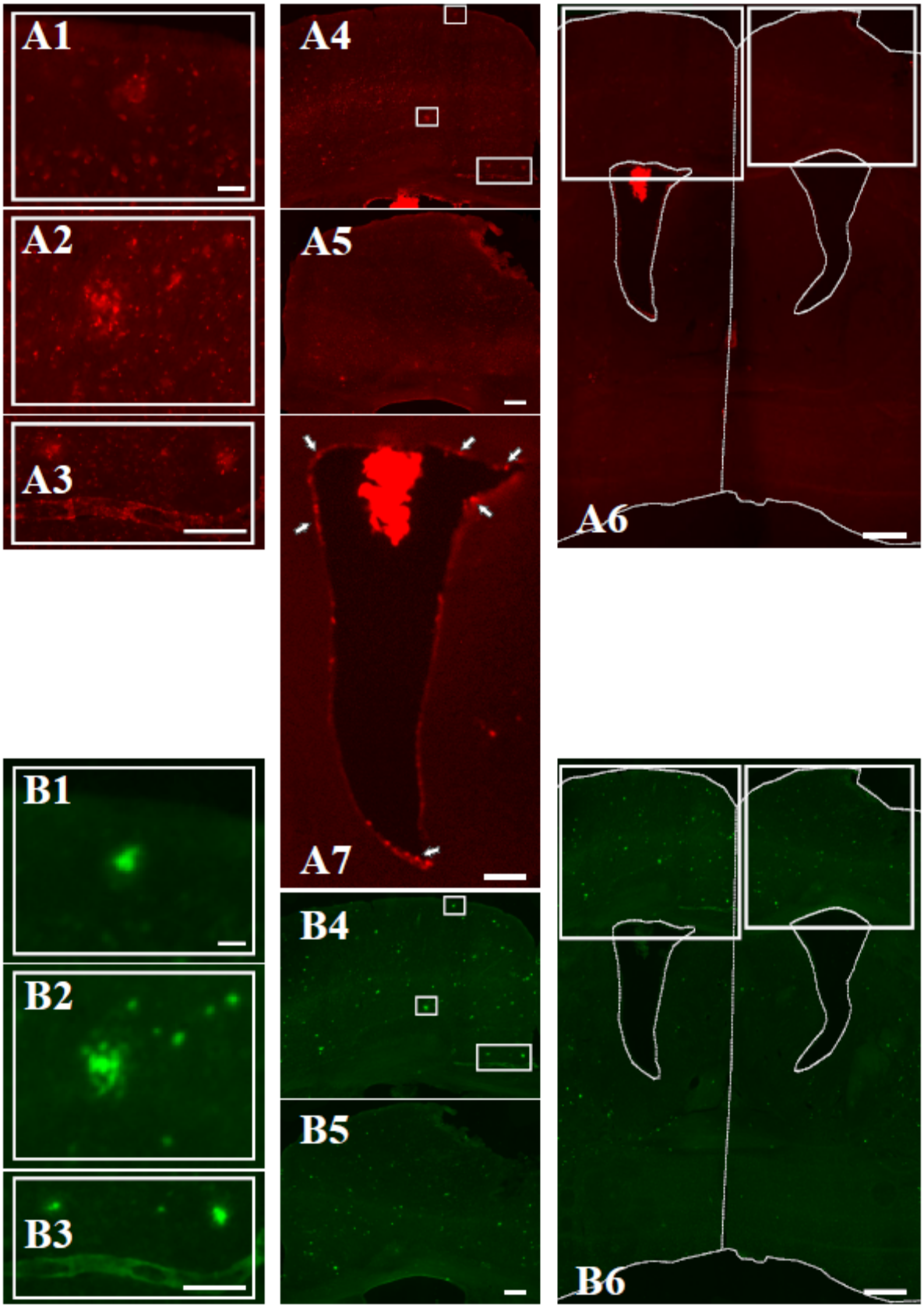

Figure 3. Representative example of spreading of TAMRA-labeled synthetic Aβ1-42 24 h after a unilateral intracerebroventricular microinjection. Note the intense fluorescence on the ventricular

wall ipsilateral to the injection site (A6, left; and A7), and weaker fluorescence contralaterally (right, A6). White frames in both A6 and B6 indicate the location of enlargements A4 & B4 (ipsilateral) and A5 & B5 (contralateral). White frames in both A4 and B4 indicate the location of further enlargements as showed in A1-3 & B1-3, respectively. Scale bar 10 µm in A1 & B1 (also applicable to A2 & B2), 200 µm in A3 & B3, 200 µm in A5 & B5 (also applicable to A4 & B4), 500 µm in A6 & B6, and 200 µm in A7.

2. *Dynamics of fluorescently labeled Aβ1-42 in vivo*

Although histology showed that fluorescently labeled Aβ1-42 penetrates brain parenchyma and clearly accumulates in the plaques, we could not fully rule out the possibility that this preferential labeling is an artefactual effect due to the sample preparation for histology. For example, brain perfusion or rinsing of brain sections may wash out synthetic Aβ from the parenchyma. Therefore, to understand the dynamics of Aβ accumulation in the brain *in vivo* we employed two-photon excitation fluorescence microscopy (TPM). TPM has number of constrains, however. Therefore, we first performed a pilot study to find the best route of application for fluorescently labeled Aβ. Although topical application of fluorescent protein is easy to do, it is not suitable for TPM, as bright fluorescence on the brain surface would prevent deep imaging. Therefore, we injected fluorescently labeled Aβ either locally into the cortical parenchyma at a depth of 400 µm (3 TG mice) or into the lateral ventricle (TG = 3, WT = 2). An additional complication was autofluorescence of amyloid plaques, which spans the entire spectrum of visual light (Kwan et al., 2009). To ensure better fluorescent signal stability over multiple recording sessions we normalized the signal intensity in the TAMRA-specific channel (590-650 nm) to the nonspecific channel (420 - 500 nm). In accordance with post-mortem histological studies, TPM showed fluorescently labeled Aβ spread throughout the brain in the course of a few hours. However, this process *in vivo* was not homogeneous in time and space as would be expected from passive diffusion (**Fig. 4** A & B). In particular, it took about 2 h from the injection for the fluorescent signal to be detectable in the TPM recording window, and during the first 4 - 8 h the fluorescent protein accumulated primarily in superficial cortical layers (0 - 100 µm from brain surface). The same pattern of fluorescence signal spread was observed in WT mice with a Dextran injection as well (n = 3). This finding suggests the existence of a route for rapid transfer of substances perpendicular to the brain surface, consistent with the recently reported 'glymphatic' paravascular (Iliff et al., 2012) or perivascular (Bakker et al.,

2016) pathways. Our recording of fluorescently labeled Aβ spreading indirectly confirms that labeled protein preferred to move next to blood vessels (**Fig. 4** C 1-3).

Although TPM yielded evidence of dynamic spread of fluorescently labeled Aβ *in vivo*, it became evident that we could not follow accumulation of Aβ in multiple plaques after an intracortical injection. The main hurdle was that despite a small injection volume and injection site as far as 500 µm away from the TPM window center, tissue geometry on injection site was distorted, making laser power adjustment for TPM a daunting task. An injection into ventricular cavities appeared as the most natural way to explore synthetic Aβ and amyloid plaque interaction. However, in that case the imaging time window had to be longer than 24 h, because fluorescence signal from the ventricles reached the cortical surface much more slowly. Unfortunately, the health of aged transgenic mice with a high enough plaque density (> 12 months) did not allow multiple anesthesias in a short time window; therefore, younger animals (9 - 10 months old) were used. Nevertheless, we were able to record successfully two APP/PS1 mice for a period up to 24 h after injection of fluorescently labeled Aβ into ventricular cavities. Our data show that 24 h after a unilateral i.c.v. injection, synthetic Aβ evenly distributes through all cortical layers (**Fig. 4** B, in magenta). Furthermore, we measured to which extent the plaque accumulates fluorescence signal as compared with its surrounding. In agreement with our histological studies, we found clear evidence of increased Aβ labeling in the plaque compared to its periphery or remaining parenchyma (**Fig. 5**, C1-2).

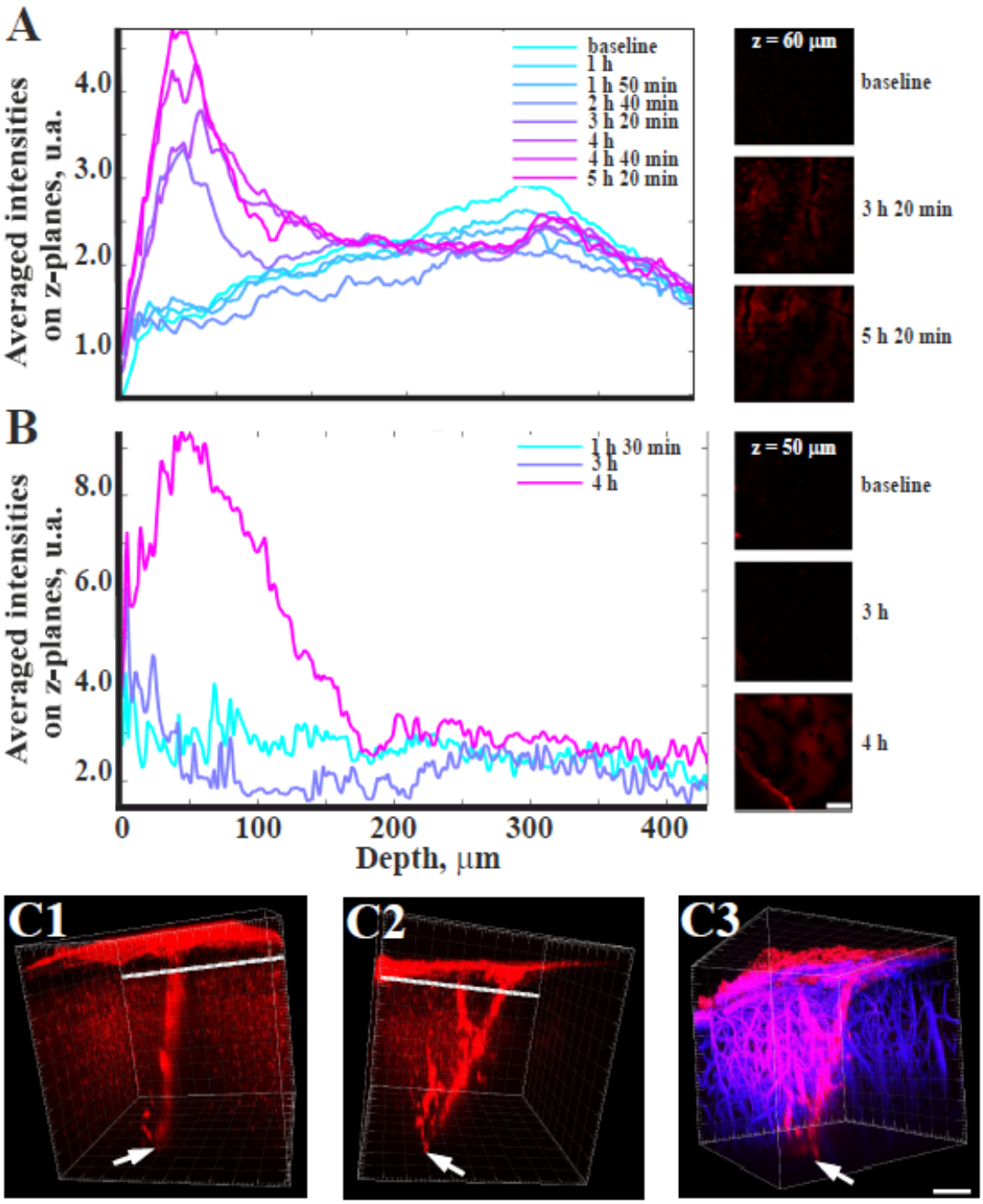

Figure 4. Dynamics of fluorescently labeled Aβ *in vivo*. (A) Graphic illustration of vertical movement of synthetic Aβ over 5 h after a unilateral i.c.v. injection. Colored lines represent corresponding time after Aβ injection. Three insets on the right show fluorescence signal in the recording window 500 x 500 µm at the depth of 60 µm. (B) As in (A) but after a local intracortical microinjection. Note that fluorescence in A & B appears stepwise: it takes at least 3 h for the fluorescent signal to be detectable in the TPM recording window, and for the first 6 h Aβ

accumulates only in the superficial cortical layers (0 - 100 µm). (C1 & C2) A TMP image shown at two angles of rotation 2 h after an intracortical injection. TAMRA-labeled Aβ signal is shown in red. (C3) Extensive staining for labeled Aβ (magenta) proximal to blood vessels (in blue; after dextran injection), but much less fluorescence in the surrounding parenchyma. White arrows in C1-3 point to the injection site. Scale bar = 10 µm.

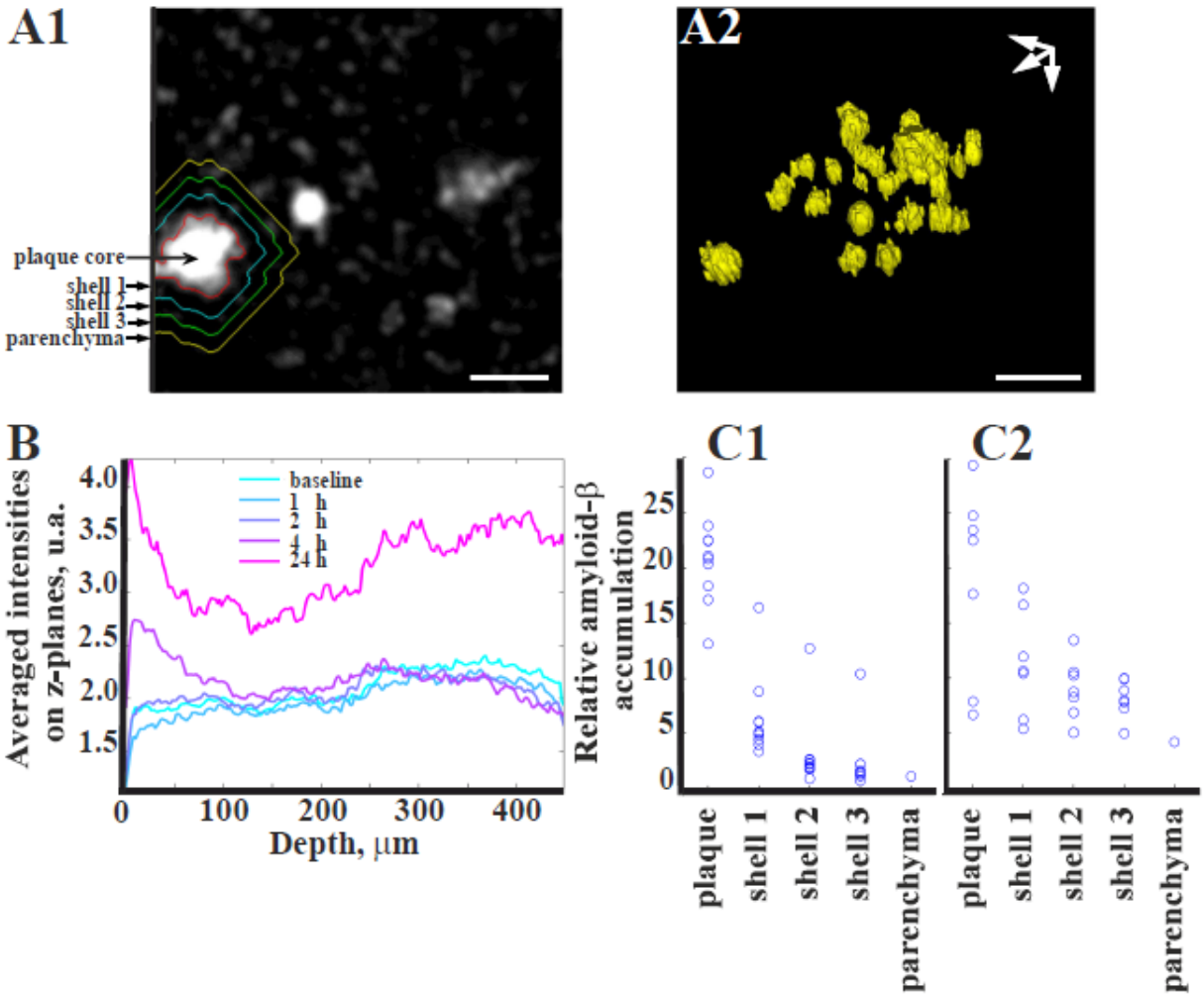

Figure 5. Fluorescently labeled Aβ accumulates in plaques more than in surrounding tissue *in vivo*. (A1) Boundaries of the plaque vs. surrounding shells as used in the assessment of fluorescently labeled Aβ accumulation gradient. (A2) 3-D reconstruction of plaques from the autofluorescence signal. (B) Graphic illustration of vertical diffusion of fluorescently labeled Aβ over 24 h after an i.c.v. injection. The specific fluorescence (total – autofluorescence recorded in the nonspecific channel) reaches only the superficial cortical layers during the first 4 h, and only 24 h later it is evenly distributed through all cortical layers. Colored lines represent corresponding time after Aβ

injection. (C1 & C2) Normalized fluorescence shows a decreasing gradient of signal from the plaque towards the parenchyma (examples from 2 different animals).

Discussion

The 'toxic Aβ oligomer' hypothesis has gained considerable support among AD researchers as a way to resolve the poor correlation between amyloid plaque load and cognitive impairment or neurodegeneration (Benilova et al., 2012). With the increasing emphasis on soluble Aβ oligomers as the culprit of AD, the role of amyloid plaques has concurrently changed from the cause of neurotoxicity to less harmful by-standers. Amyloid plaques have also been seen as an attempt of the brain to safely deposit toxic soluble Aβ species in a compact form. The present findings lend support to this notion. In particular, our histological and two-photon microscopy results show that plaques have capacity to bind additional Aβ peptide *in vivo*.

Our experiments with fluorescently labeled Aβ demonstrated that freely diffusible Aβ-peptide indeed accumulates in amyloid plaques. This is an extension of earlier work, which suggested that cerebral amyloid deposits can rapidly sequester soluble Aβ from the brain interstitial fluid (Hong et al., 2011). The earliest time point when we could demonstrate this was at 4 hours. The present findings that amyloid plaques can absorb additional labeled Aβ are in line with accumulated evidence that mature amyloid plaques still keep growing *in vivo* (Burgold et al., 2011; Condello et al., 2011; Hefendehl et al., 2011; Yan et al., 2009). It is worth noting, however, that the rate of growth of amyloid plaques in transgenic mice slows down with increasing age of the animals (Burgold et al., 2011; Yan et al., 2009). We chose 10-month-old mice with sufficient plaque density to the imaging studies to compensate the relatively poor diffusion of fluorescently labeled Aβ in aged animals. As newly formed plaques in young adult mice grow faster than in middle-age mice, they probably also absorb Aβ more efficiently. Thus, the present data in 10-month-old mice may have even underestimated the capacity of amyloid plaques to absorb additional Aβ. Our data are also in line with a recent demonstration of a concentration gradient of oligomeric Aβ around amyloid plaques in the human brain (Koffie et al., 2012). A more direct way to address the ability of amyloid plaques to bind and neutralize toxic oligomers would have been fluorescent tagging of Aβ oligomers instead of monopeptides as done here. However, this is a formidable task since the

exact molecular structure of Aβ oligomers is still debatable. One could oligomerize the fluorescently tagged Aβ, but the resulting Aβ dimer would significantly differ from the natural Aβ dimer due to the hydrophilic nature of the TAMRA tag. Such a dimer with two hydrophilic ends would hardly compare with a plain Aβ dimer that is highly lipophilic. Further, even with one added hydrophilic tag (in 1:1 ratio) the affinity of this complex to amyloid plaques should be lower than that of an Aβ dimer or monomer.

Several known mechanisms contribute to eliminating excess Aβ from the brain parenchyma. Aβ can be enzymatically degraded in the parenchyma or transported across the BBB to the blood circulation by specific transport mechanisms or through the para- and perivascular systems (Bakker et al., 2016). The present data together with earlier *in vivo* imaging studies on the kinetics of amyloid plaque growth (Burgold et al., 2011; Condello et al., 2011; Hefendehl et al., 2011; Yan et al., 2009) lend support to the notion that amyloid plaque formation may acct as a buffering system to bind toxic soluble Aβ oligomers. However, because Aβ is at an equilibrium around the plaques, also the concentration of soluble Aβ species is particularly high around the plaques (Koffie et al., 2012), which leads to local toxicity as evidenced by neuronal hyperactivity (Busche et al., 2008), dystrophy (Bell et al., 2006; Condello et al., 2011), and synaptic loss (Bittner et al., 2012; Dong et al., 2007). As the plaques grow and mature this buffering capacity is gradually lost (Condello et al., 2011). It is tempting to speculate that this coincides with the rapid deterioration of the overall brain function in the symptomatic phase of AD. This idea is in keeping with the current view of amyloid accumulation in human according to CSF biomarker studies and PET imaging: by the time the disease process leads to cognitive symptoms justifying the AD diagnosis, there is no longer significant increase in the brain amyloid load (Jack et al., 2010; Kadir et al., 2012). This hypothesis remains to be tested in future studies with infusions of toxic Aβ oligomers into plaque-loaded vs. plaque free brain tissue in transgenic mouse models.

Bakker EN, Bacskai BJ, Arbel-Ornath M, Aldea R, Bedussi B, Morris AW, Weller RO, Carare RO. Lymphatic Clearance of the Brain: Perivascular, Paravascular and Significance for Neurodegenerative Diseases. Cell Mol Neurobiol. 2016 Mar;36(2):181-94.

References

Error! Unknown switch argument.